IEEE *Access*
Multidisciplinary | Rapid Review | Open Access Journal

Optimization of the Progressive Image Mosaicing Algorithm in Fine Art Image Fusion for Virtual Reality

BIN SONG[ID]
Ceramics College, Pingdingshan University, Pingdingshan 467000, China
Faculty of Design and Architecture, Universiti Putra Malaysia, Kuala Lumpur 43400, Malaysia
e-mail: songbinbin2@163.com

ABSTRACT The fade-in and fade-out algorithm based on the Bernstein polynomial has certain limitations in image fusion. Therefore, this article proposes a new image fusion algorithm. First, the SIFT algorithm is used to register the images. Second, for the disjointed case of overlapping regions, a progressive image mosaic fusion algorithm in the form of a sine function is proposed. Finally, in order to make the progressive image mosaic fusion algorithm suitable for a variety of overlapping regions, this paper adds segmentation technology. The simulation experiment results show that the algorithm proposed in this paper is in good agreement with the spatial details and texture details of a high-resolution panchromatic image, and the time is shorter, which meets the real-time requirements. In addition, the algorithm proposed in this paper is effective in applications such as virtual reality and art image fusion.

INDEX TERMS Virtual reality, progressive image, mosaic, fine art image, fusion, SIFT, overlapping area, segmentation.

I. INTRODUCTION

In order to solve the contradiction between the field of view and the image resolution, to obtain a 360° panoramic image while maintaining the resolution, people consider using computer programs to splice the sequence images together, and image mosaicing technology [1], [2] is proposed. The characteristics of image mosaicing are effective in remote sensing, virtual reality, artistic image fusion, and other application fields [3], [4]. Image mosaicing technology is a technology that combines two or more image sequences with overlapping information taken from the same sensor and the same scene into a wide-view, high-quality panoramic image through image registration and fusion [5]–[7]. The panoramic images obtained by this technology can truly and effectively express the real world, which helps us to understand the real world more deeply. In recent years, image mosaicing technology has become a research hotspot in computer vision, virtual reality, image processing and other fields and has been widely used in many fields such as military, medical imaging, aerospace, and video surveillance.

To date, panoramic image mosaicing technology has achieved many results. For example, Cao *et al.* [8]

proposed a panoramic mosaicing algorithm that could be applied to video images. The algorithm gave the form of a plane transformation model and used the nonlinear iterative L-M algorithm to obtain its parameters to complete global registration. Peng *et al.* [9] proposed the Harris corner detection algorithm based on the Moravec algorithm. This algorithm is a local autocorrelation function algorithm that is invariant to rotation and grayscale, and the accuracy of the algorithm reaches the subpixel level. Wang *et al.* [10] proposed a cylindrical panoramic image mosaicing algorithm that projected the image to be mosaicked onto the cylindrical surface for mosaicing. The mosaic effect was good, and the algorithm has been widely used. Although the current algorithm has achieved good fusion results, there are still certain limitations:

(1) The calculation speed is slow.

(2) Some current panoramic image mosaicing technologies mostly focus on how to mosaic sequential images geometrically, and they have not achieved panoramic seamless mosaics of images.

(3) There is no better algorithm for eliminating the cumulative error when mosaicing multiple images, which is of great significance to improving the quality of mosaicked images.

Based on the above analysis, this paper proposes a new image mosaic fusion algorithm based on the analysis and

research of the Bernstein polynomial gradual in-out algorithm. Specifically, the technical contributions of our paper can be concluded as follows:

(1) The SIFT algorithm is used to register images. The feature points extracted by the SIFT algorithm remain invariant to rotation and scaling and have a strong sense of unclear illumination and noise.

(2) A progressive image mosaic fusion algorithm in the form of a sine function is proposed. This algorithm can solve the disjointed situation of overlapping areas and realize a seamless mosaic of panoramic images.

(3) Segmentation technology is added to make the progressive image mosaic fusion algorithm suitable for multiple overlapping areas. Furthermore, it can eliminate the accumulated error in the fusion of overlapping regions.

II. RELATED WORK

To date, panoramic image mosaicing technology has achieved many results. Jia *et al.* [11] proposed a more robust scale-invariant feature transform (SIFT) algorithm and applied it to image mosaicing. However, the disadvantage is that the calculation speed is slow. Pandey and Pati [12] extended image mosaics to a higher stage and proposed an image mosaic algorithm that can adaptively select the motion model, which greatly improves the matching efficiency. Cooper *et al.* [13] proposed a fully automatic image mosaicing algorithm. The algorithm can automatically identify and sort the sequence images. After the robust SIFT feature extraction algorithm is used for image registration, bundle adjustment technology is used to solve the camera parameters, and the multiresolution method is used for fusion. The algorithm has achieved a good mosaic effect, improving panoramic image mosaicing technology to a new level. Tang *et al.* [14] proposed performing image enhancement before image mosaicing so that the extracted image features would be more accurate and obvious, and this improved the image registration accuracy. Du *et al.* [15] proposed a panoramic image mosaic optimization algorithm based on a mobile camera system. The algorithm not only improves the calculation efficiency but also ensures the payment effect. Huang *et al.* [16] proposed a method to remove ghost images. The algorithm uses the human visual characteristics to find the best stitching line that can bypass the moving object or protruding part according to energy spectrum technology. By calculating the image energy spectrum and the image gray gradient, the feature points at the image stitching gap are restored and enlarged, and ghosting is eliminated. Zeng *et al.* [17] proposed a camera-based image sequence mosaicing algorithm. The algorithm does not need to calibrate the camera. The algorithm directly uses the camera to rotate around the vertical axis to shoot the sequence of images, complete the mosaic in the cylindrical coordinate system, and obtain the ideal mosaic result. Kim and Ra [18] extended the panoramic image mosaicing algorithm to a wider range of fields and proposed a dynamic panoramic image generation algorithm, which greatly enhanced the realism of images. Han and Han [19] proposed an image

mosaicing algorithm based on dynamic programming. The algorithm uses the dynamic programming method to find the best stitching line and uses the multiresolution method for image fusion to eliminate the exposure difference and solve the ghosting problem. Liao *et al.* [20] proposed an image mosaicing algorithm based on image cutting. The algorithm uses graph cutting to find the best seam to eliminate ghosting and uses the Poisson fusion of overlapping transitions to solve the exposure difference problem. Hamwood *et al.* [21] proposed a fully automatic image mosaicing algorithm to address the lack of automation of traditional algorithms. The entire mosaicing process is automatically completed, and the feature extraction is also filtered many times to ensure the registration accuracy. Adams [22] used the phase correlation method to realize the automatic sorting of out-of-order images and applied it to the mosaicing of panoramic images. The degree of automation has improved, but the method consumes considerable time. Sitara and Mehtre [23] proposed a mosaicing algorithm applied to video surveillance images, especially for some video images with motion occlusion and noise. Yong *et al.* [24] studied a panoramic image mosaicing algorithm under a cylinder and obtained a seamless panoramic image relatively quickly and effectively. Lin *et al.* [25] used the characteristics of an image in the frequency domain and the spatial domain to propose an image mosaicing algorithm that can realize automatic sorting. The algorithm is simple and effective with a high registration rate, fast speed, and good mosaic effect. Zhang *et al.* [26] studied the SURF algorithm, which is less complex and more efficient than the SIFT algorithm, and used this algorithm to mosaic panoramic images. Tang *et al.* [27] studied the mosaicing algorithm for infrared images. The algorithm combines feature registration and Poisson fusion, has good robustness, is free from noise interference, is simple and effective, and has no splicing gaps.

Through the analysis of the above algorithms, we understand that image mosaicing algorithms are very complicated. Therefore, we will introduce the relevant knowledge of image mosaicing algorithms.

III. IMAGE MOSAICING THEORY

A. THE BASIC IMAGE MOSAICING PROCESS

Image mosaicing requires a series of operations on collected sequence images and finally synthesizes a wide field of view, high-resolution, high-quality panoramic image [28], [29]. The purpose of image mosaicing is to prevent mosaic gaps in the mosaic result, that is, to achieve a seamless mosaic of images. The more "seamless" a mosaic is, the better the result. Generally, image mosaicing includes four steps, as shown in Figure 1. Among the steps, image registration and image fusion are two key steps of image mosaicing that have a great influence on the final mosaic result, so they are also the focus of this paper.

The first step of image mosaicing is image acquisition. The image sequence to be mosaicked is obtained through image acquisition, and then these image sequences
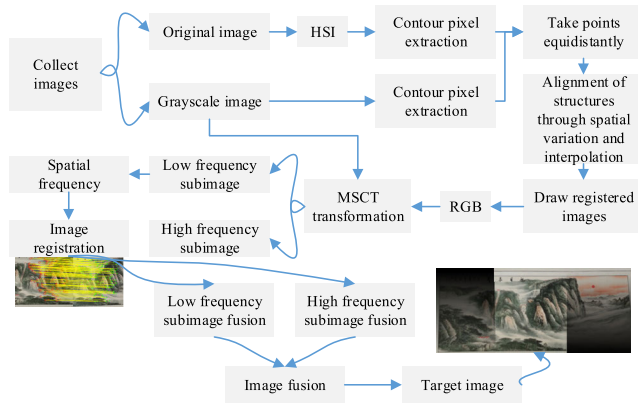
FIGURE 1. The steps of image mosaicing are image acquisition, image preprocessing, image registration, and image fusion.

are preprocessed. Then, image registration is performed on the preprocessed image sequence. A certain similarity measure is used to find the geometric relationship between the images and transform these image sequences into a unified coordinate system. Finally, a fusion algorithm is used for seamless processing to obtain a panoramic image.

Image acquisition obtains a sequence of images to be spliced with overlapping areas acquired by camera shooting. Image preprocessing mainly includes brightness correction and image projection for the images to be spliced. Among these steps, image projection can be selected from the following according to the shooting method and camera type: plane projection, cylindrical projection and spherical projection. When using a fisheye camera, you also need to correct the image. Image registration mainly conduct image feature point detection and matching, and the projection parameters of the image to be spliced are calculated by the information related to feature point registration. Image fusion uses related algorithms to merge the overlapping areas of multiple images to eliminate artificial traces in the overlapping areas.

B. COLLECTING IMAGES

Image collection obtains the original image mosaic, and the quality of the collected images directly determines the effect of the final panoramic image. Therefore, in order to obtain high-quality panoramic images, it is generally necessary to use professional equipment in the acquisition process. Because this equipment is expensive, digital cameras are often used in practice, and their low-cost acquisition methods are simple. There are many ways to collect images. According to the different camera movement methods, the collection methods are generally divided into three types: rotation, translation, and handheld shooting [30], [31].

(1) Rotary shooting

This method places the camera on a prefixed tripod, rotates the camera around its axis, and take a picture every time it rotates through a certain angle. However, it is necessary to ensure that there is a certain overlap between adjacent images.

(2) Pan shooting

In this method, the camera needs to be placed on a sliding track for sliding shooting to ensure a constant focal length between the camera and the scene. The focal length will directly affect the final mosaic effect. The photos taken via this collection method are all on the same plane. Therefore, it is suitable for simple plane mosaic models. However, the stereoscopic effect of the panoramic image obtained by this method is poor, and the shooting conditions are relatively harsh, so the practicality of the method is not high.

(3) Handheld shooting

This method only needs to hold the camera for shooting. Compared with the first two methods, this method does not require professional equipment, and the operations are simple and easy. One just holds the camera standing in place and rotates it or moves it horizontally.

When applied in actual filming, the above three methods will experience some problems, such as the change of the light source, exposure differences, the movement of the objects in the scene, etc.; these factors have certain effects on the mosaicing process. Therefore, during filming, one must move the camera with the minimum motion parallax as much as possible to prevent the occurrence of camera offset due to rotational or translational motion, jitter, and inconsistent brightness. In addition, the appropriate fusion method to eliminate exposure differences is also the focus of the study. The handheld shooting mode does not need professional equipment and is easy to operate. One just holds the camera and rotates it in place or moves it horizontally. Therefore, this paper adopts this method to collect images.

C. IMAGE PREPROCESSING

With the development of image stitching technology, traditional image stitching algorithms have achieved good results in general scenes. However, in some unconventional situations, such as changes in the shooting direction and location or the movement of the light source, there is a large difference in the brightness between adjacent images in the image sequence to be stitched, which will affect the panoramic image obtained after the image sequence is stitched. The fusion area of the image will have an obvious brightness difference such that the panoramic image does not present a consistent visual effect.

When there are images with large brightness differences in the image sequence, the image sequence needs to be optically registered. The brightness correction of the image can adjust the entire image sequence to a similar brightness level. Then, the image fusion algorithm is used for fusion, which can effectively avoid the boundary between the light and dark junctions caused by the brightness difference of the panoramic image in the overlapping area so that the final output panoramic image has an unnatural transition in the overlapping area. Therefore, in order to make the stitched image have a consistent visual effect, brightness correction processing of the stitched image must be performed.
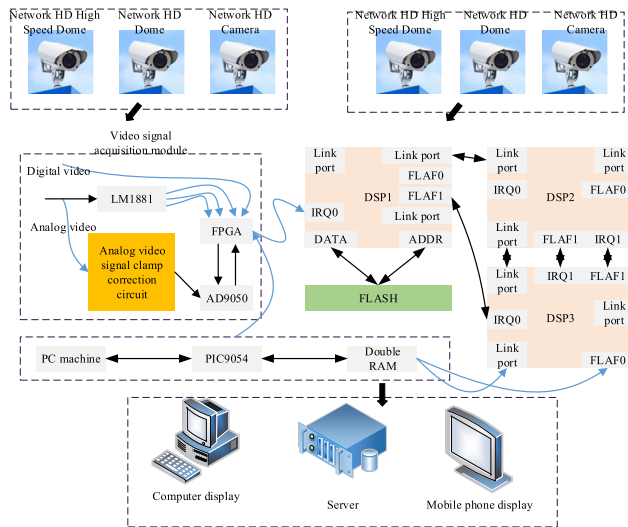
FIGURE 2. An image acquisition device that uses multiple cameras to take images and upload the images to the server for processing.

D. IMAGE REGISTRATION

(1) SIFT feature detection

The core of the SIFT algorithm is to find extreme points in different scale spaces and calculate and extract the positions, scales and directions of the extreme points. Since the feature points extracted by the SIFT algorithm remain invariant to rotation and scaling and have strong robustness to illumination and noise, they are widely used in image feature detection and matching. The main process is as follows:

1) Build a scale space

2) Detect the extreme points

3) Specify the direction for feature points

4) Construct a feature point descriptor

(2) SURF feature detection

The SURF algorithm is an improved algorithm based on the SIFT algorithm, and its general steps are similar to those of the SIFT algorithm. The process of establishing the descriptor is shown in Figure 3.

(3) ORB feature detection

The ORB algorithm is a BRIEF descriptor of the orientation of FAST feature points and rotation.

1) Oriented FAST

The main idea of fast feature points is to compare the target pixel with the pixel on the circular boundary of its neighborhood. When there are multiple connected pixels on a circle and the absolute difference between the target pixels exceeds the threshold, the target pixel is selected as the key point.

2) Rotated BRIEF

The main idea of the BRIEF feature descriptor is to select n pairs of pixels in a circular neighborhood centered on the feature point and compare their gray values. When n pairs of pixels are compared, a binary string of length n is generated as the descriptor of the feature point.

The BRIEF descriptor occupies a small amount of memory and is fast, but it does not have directionality. Therefore,
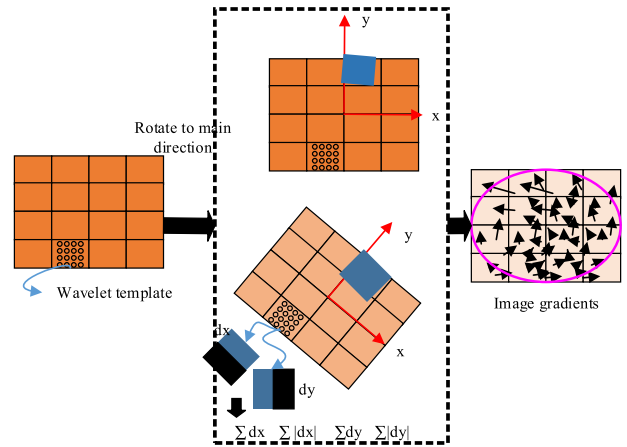

FIGURE 3. The establishment of the SURF feature descriptor: The box filter is used to approximate the second-order Gaussian function in the SIFT algorithm, and then the image is convolved.

the BRIEF descriptor cannot describe the directional information of the feature points. Due to the adjustment of the directionality of the BRIEF descriptor, the relevance of random point pairs increases and the discriminative decreases, which reduces the discriminability of the descriptor. You can use brute force and exhaustive methods to find point pairs with less correlation.

E. IMAGE FUSION

Image fusion [32]–[37], which is the calculation and processing of the overlapped area of the image after alignment, is a key step of image stitching.

(1) Direct average method

This method will simply add the gray values of the overlapping parts of the image and then average the results. However, it will make the image mosaic have obvious traces. The process is described as follows:

Let I1 and I2 represent two images to be mosaicked. I is used to represent the fused image. The variable a represents the row coordinates of the image, and b represents the column coordinates of the image. They have the following relationship, as shown in formula (1).

$$I(a, b) = \begin{cases} I_1(a, b) \\ (I_1(a, b) + I_2(a, b))/2 \\ I_2(a, b) \end{cases} \quad (1)$$

(2) Weighted average method

The idea of the weighted average algorithm originated from the direct average method, which is an effective improvement to the direct average method. This method can make the image mosaic result smoother, and it can effectively eliminate mosaic gaps in the image. This method is now widely used and is shown in formula (2). λ1 and λ1 represent the weights of image I1 and image I2, respectively.

$$I(a, b) = \begin{cases} I_1(a, b) \\ (\lambda_1 I_1(a, b) + \lambda_2 I_2(a, b))/2 \\ I_2(a, b) \end{cases} \quad (2)$$

(3) Median filtering method

This method is the median filtering of the overlapping parts of the image. Under certain circumstances, this method can overcome the situation where the image may have blurred details.

(4) Pyramid fusion method

This method first performs a series of multiresolution decompositions on two images to be mosaicked. This technology first decomposes the resolution of images and then performs image fusion. This method can effectively fuse the contents of images and make the fusion result very smooth.

Due to some objective factors in the acquisition of images, the images to be spliced cannot be perfectly aligned in the overlapping area, and direct splicing will result in ghostly images and obvious splicing traces in the overlapping area. The purpose of the image fusion algorithm is to process overlapping areas, eliminate ghost shadows and artificial traces, make the mosaicked image more natural, and improve the mosaic effect. Therefore, image fusion technology is embedded into image mosaic technology in this paper. First, the SIFT algorithm is adopted to register the image in this paper. Second, the sine function form of the progressive image mosaic fusion algorithm is proposed for the case of overlapping regions not intersecting. Finally, segmentation technology is added to make the progressive image mosaicing fusion algorithm suitable for a variety of overlapping areas.

IV. IMAGE FUSION ALGORITHM BASED ON PROGRESSIVE IMAGE MOSAICING

First, the SIFT algorithm is adopted to register the image in this paper. Second, the sine function form of the progressive image mosaicing fusion algorithm is proposed to solve the problem of overlapping regions not intersecting, which makes the method more practical and applicable. The method can be used in virtual reality, art image fusion and other applications. Finally, segmentation technology is added to make the progressive image mosaicing fusion algorithm suitable for a variety of overlapping areas, which makes the algorithm a convenient and flexible image mosaicing fusion algorithm.

A. SIFT IMAGE REGISTRATION METHOD

The core of the SIFT algorithm is to find extreme points in different scale spaces and calculate and extract the positions, scales and directions of the extreme points. Since the feature points extracted by the SIFT algorithm remain invariant to rotation and scaling and have strong robustness to illumination and noise, they are widely used in image feature detection and matching. Therefore, this paper chooses the SIFT algorithm for system registration. The main process is as follows:

(1) Build a scale space

In each layer of the Gaussian pyramid, a Gaussian (a, b, c) with different blur parameters is used to convolve the source image $I(a, b)$ to obtain images with different degrees of blur in the same layer, namely, the Gaussian scale space. The mathematical expression of the Gaussian scale space

function $S(a, b, c)$ is shown in equation (3).

$$S(a, b, c) = Gaussian(a, b, c) \times I(a, b) \quad (3)$$

$$Gaussian(a, b, c) = (1/2\pi c^2) \times e^{-(a^2+b^2)/2c^2} \quad (4)$$

where G(a, b, c) is the Gaussian kernel function, and $\times$ is the convolution operation, as shown in formula (4).

Among the variables, a and b are the space coordinates of the image; the change in the degree of image blur is determined by the standard deviation of the Gaussian kernel function, which is c. As the value of c increases, an image becomes blurred, and the image details gradually disappear.

The Gaussian scale space is used to construct the difference of the Gaussian scale space, that is, the Gaussian difference pyramid. The Gaussian difference pyramid is obtained by subtracting two adjacent layers in each group of Gaussian pyramids, as shown in equation (5). Among the variables, k is the kennel size.

$$DOG = (Gaussian(a, b, kc) - Gaussian(a, b, c)) \times I(a, b)$$
$$= S(a, b, kc) - S(a, b, c) \quad (5)$$
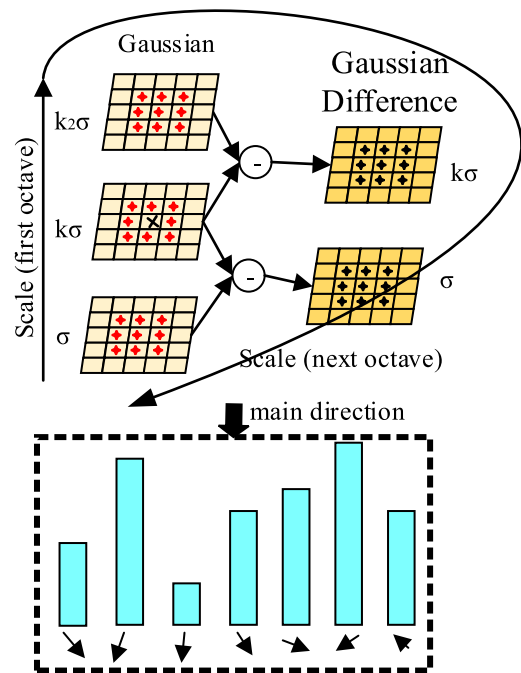
The schematic diagram is shown in Figure 4.

FIGURE 4. The Gaussian scale space is obtained by subtracting two adjacent layers in each group of the Gaussian pyramid to construct the Gaussian difference scale space.

(2) Detect extreme points

By comparing every pixel point in the Gaussian difference scale space with all the pixel points in its neighborhood, when the pixel point is the extreme value point, it is retained in the Gaussian difference scale space.

Since the discrete space is the sampling of the continuous space, the initial extremum may not be the location of the real extremum, so it is necessary to use the fitting function

in the three-dimensional space to find the real coordinates of the extremum and the number of layers in the scale space where it is located. In addition, as the Gaussian difference scale space has a strong response to the image edge, in order to improve the robustness of feature points, it is also necessary to judge and screen the extreme points after determining the real position of the extreme points so as to remove the extreme points with low contrast and unstable extreme points on the edge.

The Taylor expansion of the Gaussian difference scale space is shown in equation (6). Among the variables, a is the gray value of the image. DOG represents the initial Gaussian difference pyramid.

$$DOG(a) = DOG + a \times \partial DOG^T / \partial a \\ + \frac{1}{2} a^T a \partial^2 DOG^T / \partial a^2 \quad (6)$$

Let the derivative value of equation (6) be zero and obtain the exact position of the extreme point, as shown in equation (7). Among the variables, a' represents the exact position of the extreme point.

$$a' = -(\partial^2 DOG^T / \partial a^2) \times \partial DOG^T / \partial a \quad (7)$$

Incorporating formula (7) into formula (6), we obtain:

$$DOG(a') = DOG + \frac{1}{2} \partial^2 DOG^T / \partial a^2 \quad (8)$$

The Hessian matrix is shown in equation (9).

$$Hessian = \begin{pmatrix} DOG_{aa} & DOG_{ab} \\ DOG_{ab} & DOG_{bb} \end{pmatrix} \quad (9)$$

Let α and β be the two eigenvalues of the Hessian. Then, the trace and determinant of the Hessian matrix are calculated using equations (10) and (11), respectively.

$$Tr(Hessian) = DOG_{aa} + DOG_{bb} \\ = \alpha + \beta \quad (10)$$
$$Det(Hessian) = DOG_{aa} \times DOG_{bb} \\ = \alpha \times \beta \quad (11)$$

Let $\alpha = r\beta$. Then, we can obtain formula (12).

$$\frac{Tr(Hessian)^2}{Det(Hessian)} = \frac{(\alpha + \beta)^2}{\alpha \beta} \\ = \frac{(r\beta + \beta)^2}{r\beta^2} = \frac{(r+1)^2}{r} \quad (12)$$

Among the variables, r is the threshold. The paper recommends that r be set as 10 as the default value and judge formula (13). If the relationship is satisfied, the point is an effective extreme point; otherwise, the point is an edge response point, which needs to be removed. Tr represents the rank of the Hessian matrix. Det represents the value of the Hessian matrix.

$$\frac{Tr(Hessian)^2}{Det(Hessian)} < \frac{(r+1)^2}{r} \quad (13)$$

(3) Specify the direction for the feature point

In order to make the feature points insensitive to image rotation, that is, to have the characteristic of rotation invariance, the SIFT algorithm assigns a value to the direction of each feature point. The SIFT algorithm determines the direction of the feature point according to the gradient distribution of the pixels in the neighborhood of the feature point. The modulus $q(a, b)$ of the gradient at the pixel point (a, b) is shown in equation (14), and its direction is defined as $p(a, b)$ in formula (15). The variables l(a+1, b), l(a−1, b), l(a, b)+1 and l(a, b−1) represent the directional gradient value of each feature point.

$$q(a, b) \\ = \sqrt{(l(a+1, b) - l(a-1, b))^2 + (l(a, b) + 1 - l(a, b-1))^2} \quad (14)$$
$$p(a, b) = \arctan \frac{l(a+1, b) - l(a-1, b)}{l(a, b) + 1 - l(a, b-1)} \quad (15)$$

(4) Construct the feature point descriptor

The feature point descriptor is a summary of the feature point and its neighborhood information, mainly including the location, scale, and direction of the feature point.

In order to ensure the rotational invariance of the feature point, the feature point is taken as the center, the coordinate axis is rotated according to the main direction of the feature point, and an 8×8 window is selected in its neighborhood. In the figure, each square represents a pixel in the neighborhood of the feature point. The arrow in the square represents the gradient direction of the pixel, and the length of the arrow represents the magnitude of the gradient mode of the pixel. The pixels in the 4×4 grid are counted, a gradient histogram with 8 directions is drawn, and each 4×4 grid is called a seed point. Using the vector information of the four seed point gradient histograms, a 32-dimensional SIFT feature descriptor can be generated.

B. TRIGONOMETRIC FUNCTION ASYMPTOTIC MOSAICING ALGORITHM

In the image mosaic process, if the overlapped area of the image is simply superimposed, it will cause image blur and obvious boundaries, which cannot meet the needs of the application. In order to improve the mosaic quality, the commonly used classic method is to use the in and out fading method, that is, slowly transition from the previous image to the second image in the overlapping part and then delete the part of the image that is staggered vertically.

Assume that I3 is the overlapping part of the mosaicked image, that Il and I2 correspond to the overlapping parts of the two images, respectively, and that the variable m is used as the image gradient coefficient, where m∈[0,1]. Then:

$$I_3 = (1 - m)I_1 + mI_2 \quad (16)$$

Here, m should gradually change from 0 to 1. Therefore, the simplest and most effective way is to set m = index/width, where index is the corresponding number of columns in the
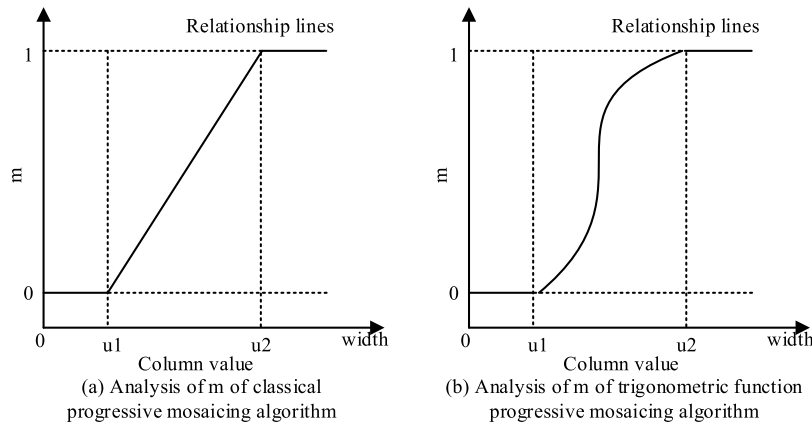
FIGURE 5. The analysis curve diagram of the value of m of the classic progressive mosaicing algorithm and trigonometric function progressive mosaicing algorithm.

overlapping area, and width is the width of the overlapping area.

Take any column in the overlapping area and analyze its m to obtain the curve in Figure 5(a).

This curve describes the correspondence between the image column direction and its corresponding value a. It is easy to see from the curve that two discontinuities of the second type appear at u1 and u2. These two discontinuities will cause sudden changes in the brightness of the image in the directions of columns u1 and u2 and visually cause image stitching.

Through the above analysis of the value of m, the original algorithm is improved, and another curve is found to replace the straight line between u1 and u2 to eliminate the discontinuity.

Assume that the trigonometric function that satisfies the conditions is as shown in formula (17).

$$m = \lambda \, sin \, (\pi/3 \times u + \pi/2) + 0.9 \qquad (17)$$

The relationship curve between m and u is shown in Figure 5(b):

In order to reduce the complexity, the u value is transformed first. Shift u1 to the origin and then stretch the interval [u1, u2] to the interval [0, 1] to obtain the new value u'. According to the conditions, it can be solved as shown in formula (18).

$$m' = 0.5 \times sin(\pi \times u' - \pi/2) + 0.5 \qquad (18)$$

In fact, u' is the original value of m. In this way, u does not need to be inversely transformed, and m' is used to replace m in the original algorithm.

The above algorithm cannot guarantee the smooth transition of the image in the other direction when the overlap area of the original image does not meet the requirement of full rows or columns. For this reason, we further consider the use of weight statistics to make it possible to meet the smooth transition in the two-dimensional direction at the same time.

First, suppose there is an algorithm. When the pixel is close to the left or right boundary, it reflects the gradual left and right progress. When it is close to the upper or lower boundary, it reflects the gradual the upper and lower progress and then realizes the two-dimensional transition. Therefore, we consider using the weighting factor t to superimpose the progressive formulas in the two directions.

For the convenience of the description, set the progressive formula for the up and down directions as ud, the progressive formula for the left and right directions as rl, and the total formula as S. Then, we can obtain formula (19).

$$S = t \times ud + (1 - t) \times rl \qquad (19)$$

In the formula, t is the percentage of the weight of the pixel point in the overlapping area to the total weight. Suppose the row weight is t_i and the column weight is t_j. Then, $t = t_i/(t_i + t_j)$.

From the above formula, we can see that when the pixel point tends to the left or right boundary, t_i should tend to 0. When the pixel point tends to the upper or lower boundary, 1-t should tend to 0, so t_j tends to 0. Thus, the drawn t_i and row relationship curve are shown in Figure 6.

Similarly, in order to reduce complexity, first, the mappings $c_1 = (u - u_1)/(u_2 - u_1)$ and $c_2 = (v - v_1)/(v_2 - v_1)$ are performed. The available functions are shown in formula (20) and formula (21).

$$t_{c_1} = \begin{cases} 0 & c_1 < 0 \\ 2 \times c_1 & c_1 \in [0, 0.5] \\ 2 \times (1 - c_1) & c_1 \in [0.5, 1) \\ 1 & c_1 > 1 \end{cases} \qquad (20)$$

$$t_{c_2} = \begin{cases} 0 & c_2 < 0 \\ 2 \times c_2 & c_2 \in [0, 0.5] \\ 2 \times (1 - c_2) & c_2 \in [0.5, 1) \\ 1 & c_2 > 1 \end{cases} \qquad (21)$$

At this time, tc1 and tc2 can already reflect the nature of the transition on the boundary. However, there may be a sudden change on the diagonal because of a discontinuity at point (0.5, 1). Therefore, replacing the original function with a parabola to eliminate this discontinuity is considered.
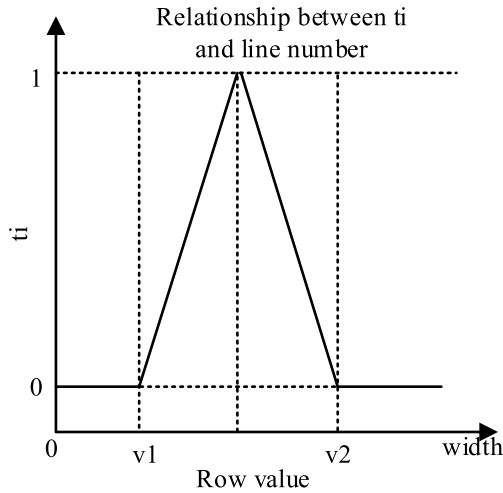
FIGURE 6. Analysis of the m-value of the two-dimensional progressive mosaic algorithm.

Figure 7(a) is the ideal parabola analysis diagram of the value of a.

In the same way, first, c1 and c2 are mapped, and the parabola is set. It is easy to find the results according to the conditions, as shown in formula (22) and formula (23).

$$t_{c_1} = -4 \times c_1^2 + 4 \times c_1 \qquad (22)$$

$$t_{c_2} = -4 \times c_2^2 + 4 \times c_2 \qquad (23)$$

In practical applications, in order to make the image stitching seam look more natural, once again, a trigonometric function is considered to replace the original function. Here, a half-wave sine function is used to remove the discontinuity at both ends. Figure 7(b) is the analysis diagram of the value of a using the half-wave sine function.

C. GRADIENT IMAGE FUSION MOSAIC METHOD

The aforementioned algorithm is only for image mosaics of intersecting relationships. If the algorithm is further modified to satisfy the image mosaic of the inclusion relationship, it will not only expand its practicality but also produce a special artistic effect. Therefore, this paper proposes an image fusion mosaicing algorithm.

Generally, image fusion performs image operations on two images with different characteristics so that the fused image reflects the characteristics of the two images at the same time [38]–[40]. However, sometimes, in order to obtain some special artistic effects or meet some special needs of image processing, the fusion area of the two images gradually transitions from the characteristics of one image to the characteristics of another image from the periphery to the center. This effect is not only different from general image fusion but is also different from edge feathering and has unique characteristics.

One approach is to use iteration. First, the two images are mosaicked, and then the mosaicked image is used as an image mosaic with another image. The images are mosaicked from left to right or top to bottom in sequence. However,

this is only feasible when the overlapping regions do not intersect, and the situation in practical applications is much more complicated.

In order to solve the above problems, a solution is proposed, and the overlapping area is divided into several rectangles. Then, the new algorithm is applied to smooth each rectangle separately. However, the following two issues should be considered when dividing the overlapping area:

(1) The number of divided rectangles should be as few as possible, and the area of the rectangles should be as large as possible.

(2) The transitional nature of the region after division may change. For example, if the overlapping area is obtained through the intersecting relationship, it may become an area containing the relationship after division.

V. EXPERIMENTAL VERIFICATION
A. EXPERIMENTAL DATA DESCRIPTION
For the convenience of the display and evaluation, the images used in this article are multiple art images crawled from the Internet. The size of the selected art image is 1550 × 1200 pixels. There are 20,000 images. These images are artistic images. The computer is configured with Windows XP, an Intel Ivy Bridge processor, a DDR3-1600 memory interface, 4 GB of running memory, and an i965 motherboard as the simulation platform.

In this paper, the number of local points and the algorithm time consumption are used as evaluation indexes for the elimination effect of matching points. In order to analyze the performance of art image fusion, this paper evaluates and analyzes the image color difference and gradient difference, as well as the degree of image texture information retention. Among these measures, the color difference refers to the reduction of the fusion results to the same spatial resolution as the original multispectral image, and the difference value is compared with the multispectral image. The gradient difference refers to the difference between the gradient of the intensity or brightness component of the fused image and the gradient of the high-resolution panchromatic image.

B. COMPARISON OF IMAGE REGISTRATION METHODS
Since the original image has considerable noise, the image needs to be preprocessed, and the result after equalization through the histogram is shown in Figure 8.

In order to verify the effectiveness of the SIFT algorithm for image registration, this paper compares the results of the SIFT algorithm, the Forstner algorithm, the SUSAN algorithm and the Harris algorithm on the same image.

First, different registration algorithms are used to perform feature detection on the image, and the image is detected multiple times by setting different window sizes and thresholds. The experimental data are shown in Figure 10.

The experimental data in Figure 10(a) show that the threshold size of the Forstner algorithm has little effect on the number of feature points detected, and the size of the window has a greater impact on the number of feature points.
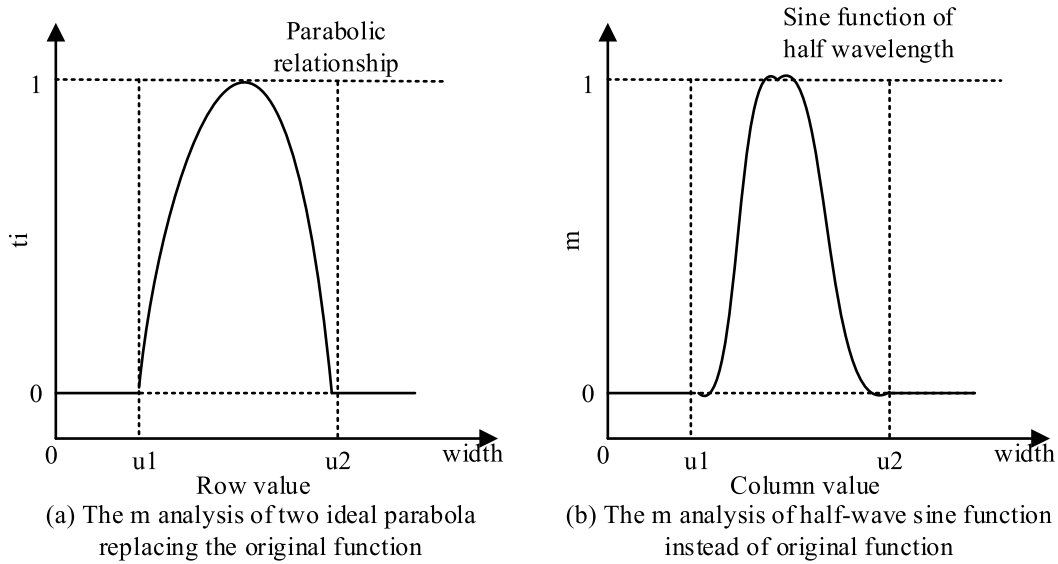
(a) The m analysis of two ideal parabola
replacing the original function

(b) The m analysis of half-wave sine function
instead of original function

FIGURE 7. The analysis curve of the value of m of the ideal parabola and half-wave sine function instead of the original function.
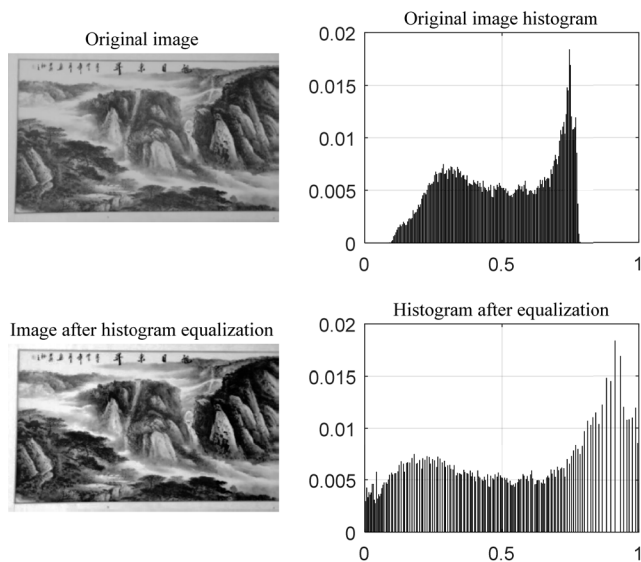

FIGURE 8. Visualization results after image preprocessing and the corresponding gray value comparison.

In addition, the larger the window size is, the smaller the number of feature points. The detection times for Forstner operators with different size windows and different thresholds are similar.

Figure 10(b) shows the experimental results using the SUSAN algorithm. As the size of the template increases, the number of feature points within the same threshold range shows an increasing trend, and the detection time decreases. The selection of the window size has a small impact on the number of feature points, and the selection of the threshold range has a greater impact on the number of feature points. When changing the window size, attention should be paid to changing the threshold range to achieve the detection effect.

The experimental data in Figure 10(c) show that according to the detection results of the Harris algorithm, when the threshold is constant, the smaller the template size of the Harris operator is, the greater the number of feature points that are detected. When the window size is constant, the larger the threshold is, the fewer the number of feature points detected by the Harris operator. The greater the number of feature points that are detected, the more time it takes for detection. The choice of threshold has a greater influence on the number of detected feature points than the choice of template size. When using the Harris operator, attention should be paid to the combination of template and threshold to achieve the best extraction effect.

The experimental data in Figure 10(d) show that when the scale space is 5 groups, the SIFT algorithm detects the largest number of feature points in the image, and the detection time is the least. As the scale space increases, the number of detected feature points also increases. This shows that the larger the template size in the scale space is, the fewer feature points will be detected. Generally, 4-5 layers of scale space search can meet the needs of feature point detection.

In order to better illustrate the effectiveness of the SIFT algorithm in detecting feature points, Figure 11 shows the number of feature points detected by each algorithm. The figure shows that the SIFT algorithm detects the most feature points and takes the least time.

Figure 12 shows the feature point detection of the same image using four feature detection algorithms. By analyzing the experimental results, the Forstner algorithm has a faster calculation speed, but the accuracy is not high. It is not sensitive to the edges and inflection points of the detection target, and it is susceptible to the influence of noise, which will produce a large number of incorrect feature points. In addition, the appropriate window size and threshold range need to be
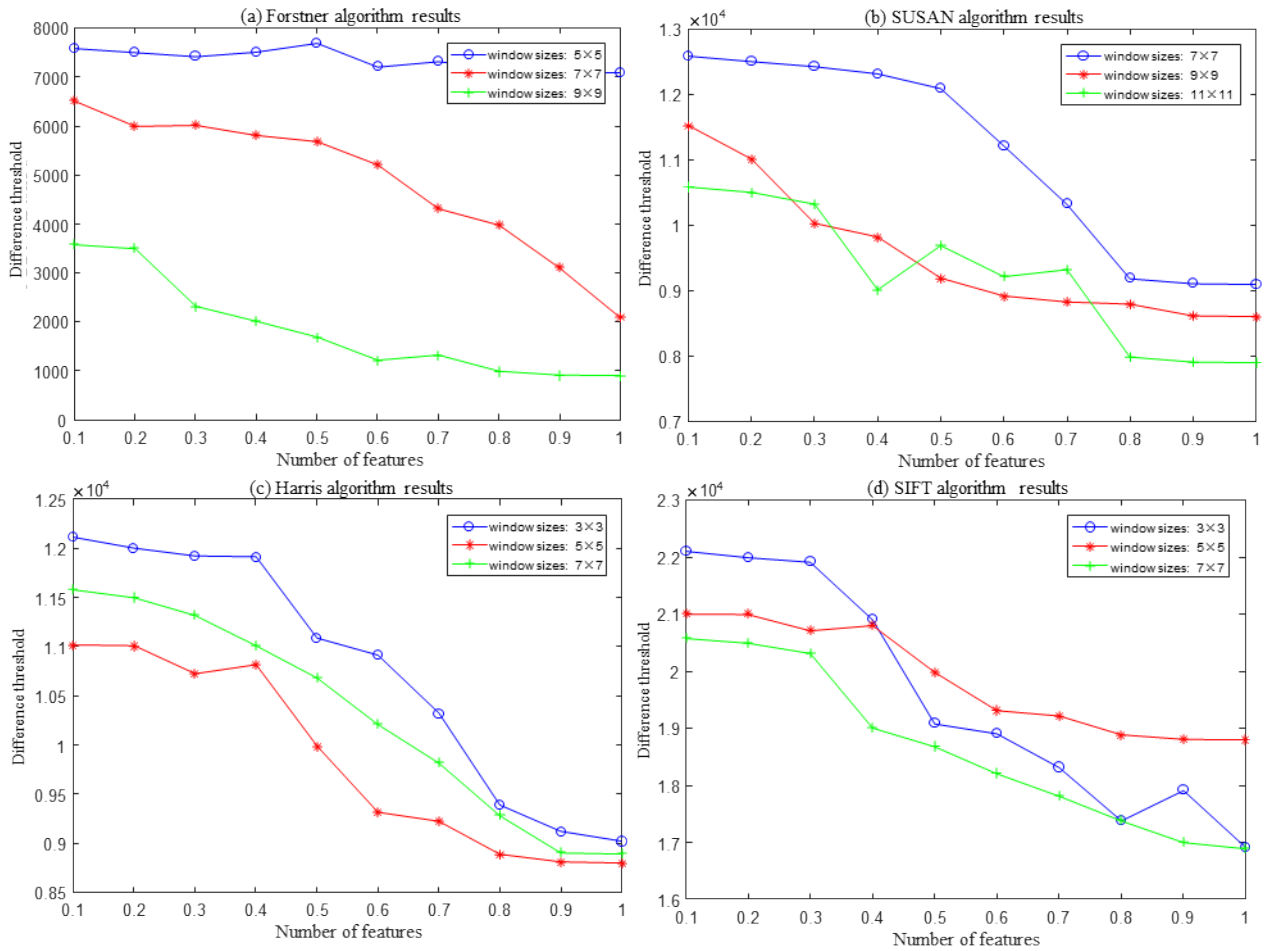
FIGURE 9. For the same image, the Forstner algorithm, SUSAN algorithm, Harris algorithm and SIFT algorithm are used to compare the feature detection results.
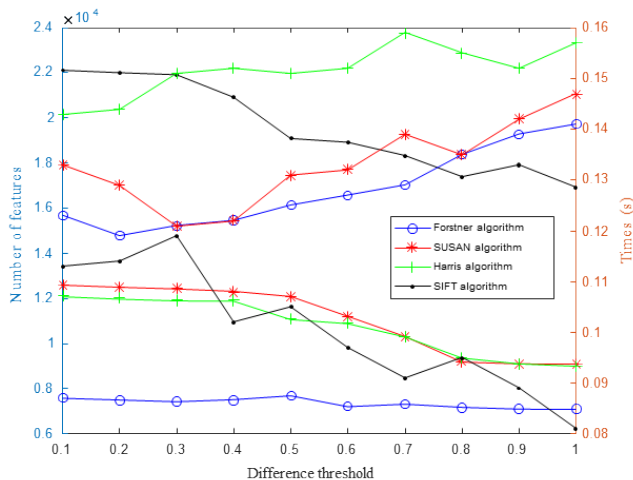

FIGURE 10. Comparison of the number of feature points detected by different algorithms and the time used by different algorithms.

determined through continuous experimentation. When the SUSAN algorithm is used to extract image features, it has a poor ability to extract the edge of the image and is more suitable for extracting the inflection point of the image target edge.

Furthermore, there is no need to derive the image, and the algorithm has a strong anti-noise ability. However, it is difficult for the algorithm to detect the correct corner points on weak edges. The Harris algorithm has high accuracy in detecting corners. However, the number of corner points extracted by the Harris algorithm is related to the texture information of the image. In areas with rich texture information, the Harris algorithm can detect more feature points. In addition, its edge detection effect is better. In areas with less texture, fewer feature points are extracted, and image feature information is easily missed. The feature points of the SIFT algorithm are concentrated around the target, and feature points are also detected for areas with weak texture information. This indicates that the SIFT algorithm has good robustness; its basic calculation speed is also the fastest of the four algorithms, which greatly improves the work efficiency. The feature points extracted by the SIFT algorithm have feature descriptors, and the local invariant features of some feature points are used to match with the feature space, which avoids the direct manipulation of image gray levels and is more robust.
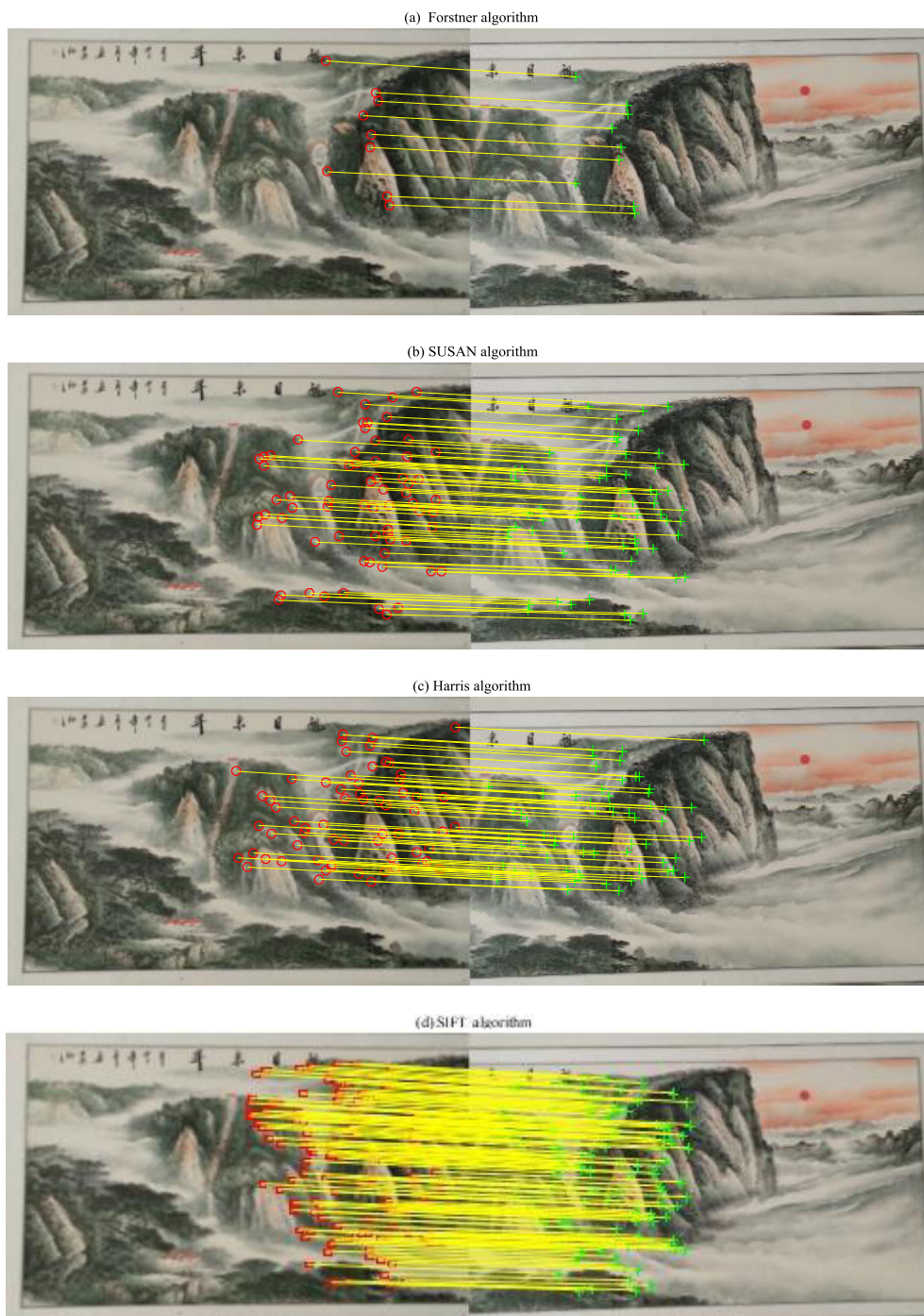
(a) Forstner algorithm

(b) SUSAN algorithm

(c) Harris algorithm

(d) SIFT algorithm

FIGURE 11. Visualized results of feature point detection using the four feature detection algorithms to perform feature point detection on the same image.

C. EXPERIMENTAL ANALYSIS OF THE MISMATCH POINT ELIMINATION ALGORITHM

We conduct an experiment with the feature points of an image using the feature points after setting the slope and threshold constraints of the two algorithms. The number of feature points is 149, and the result is shown in Figure 12.

The data in Figure 12 show that under the same constraints, the algorithm in this paper obtains 59 interior points, and

the calculation takes 0.012 s. The number of interior points obtained by the partial least square method is 43, and the calculation takes 0.197 s. The algorithm in this paper has performed multiple iterative calculations on the coordinate point data to obtain the best model with a small amount of data. The number of iterations did not substantially affect the calculation speed of the algorithm in this paper. The calculation time is much less than that of the partial least
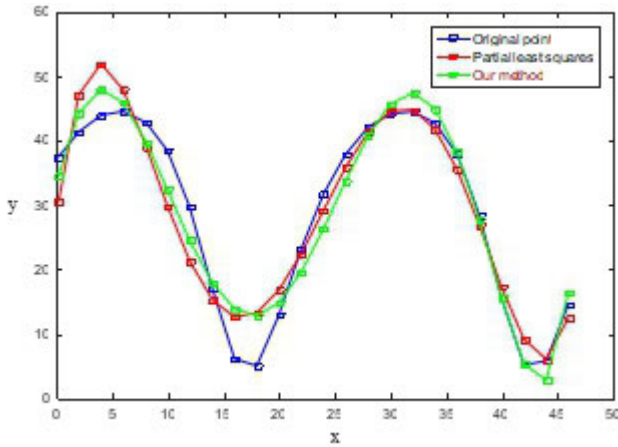
FIGURE 12. The feature points of the two algorithms after setting the slope and threshold constraints. The figure shows the feature point removal effect diagram of an image.

FIGURE 13. Data statistics of the color difference and gradient difference. The larger the color difference is, the more spectral information the image changes after fusion. The smaller the gradient difference is, the better the fused image retains the details of the high-resolution panchromatic image.

squares algorithm, and the number of interior points obtained is larger than that if the partial least squares method, so the calculation efficiency is high.

The fitting result of the partial least squares method considers the positions of all the feature points to obtain the straightest line. Although these feature points are feature points that remain after a large number of mismatched points have been eliminated, there are still some data points with relatively large errors; therefore, the obtained function model will deviate from the actual data, thereby increasing the error of the model and reducing the detection accuracy. For the matching point pairs of the strip image obtained after using the slope distance constraint, there are a large number of correct feature point pairs, but there are still some abnormal data points that make the partial least squares algorithm deviate from the actual function model. In summary, the algorithm in this paper has a better effect on purifying image feature points.

D. PERFORMANCE ANALYSIS OF FINE ART IMAGE FUSION

The statistical graph in Figure 13 can basically reflect the fusion effect between fusion algorithms. The greater the color difference is, the more spectral information the image changes after fusion. The smaller the gradient difference is, the more effectively the fused image can retain the details of the high-resolution panchromatic image. The results show that although the progressive mosaicing fusion algorithm proposed in this paper corrects the details of the image color, the degree of color difference is still close to those other fusion methods. Furthermore, the degree of retention of image gradient information or detail information is optimal.

In order to further prove the degree of image texture information retention, this paper uses a two-dimensional Gabor filter to extract the fused image texture feature value and the high-resolution panchromatic image texture feature value for the difference calculation to evaluate the degree of texture feature retention of the fused image. If the difference is smaller, it indicates that the fusion method retains more texture information.
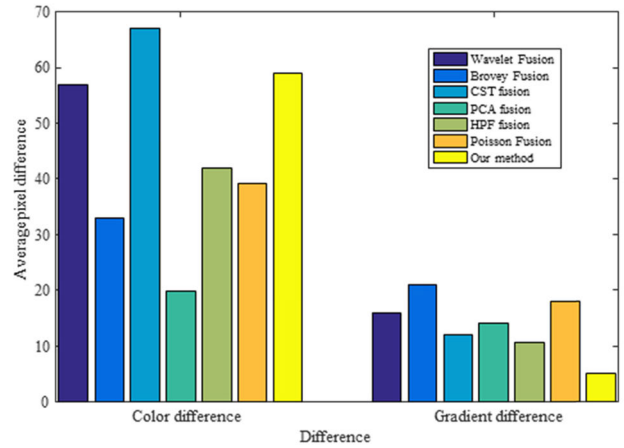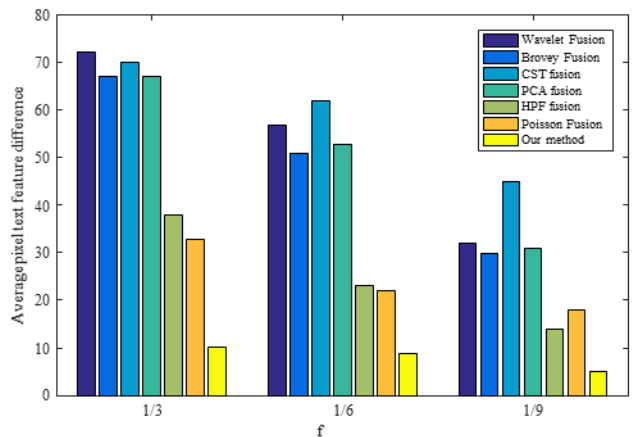

FIGURE 14. A statistical map of the difference in the texture features obtained from fused images of different methods and high-resolution images at three extraction frequencies.

Figure 14 is a statistical diagram of the difference between the texture features of the fused image and the high-resolution image of each method at 3 extraction frequencies. The quantitative analysis results prove that compared with any method, the progressive mosaicing fusion method proposed in this paper has the advantage of retaining more complete texture information in each frequency band.

Through subjective analysis of the various fused images in Figure 15, the better fusion methods include wavelet fusion, Brovey fusion and the progressive image mosaicing fusion algorithm proposed in this paper. The effect of wavelet fusion is obviously not ideal, and the color of the Brovey fusion image is seriously dark. Moreover, the wavelet fusion image and the Brovey fusion image only have a fusion effect and have no splicing effect. However, the algorithm in this paper can not only give clear geometric contour edges, but it can also obtain more realistic colors and achieve the effect of splicing.
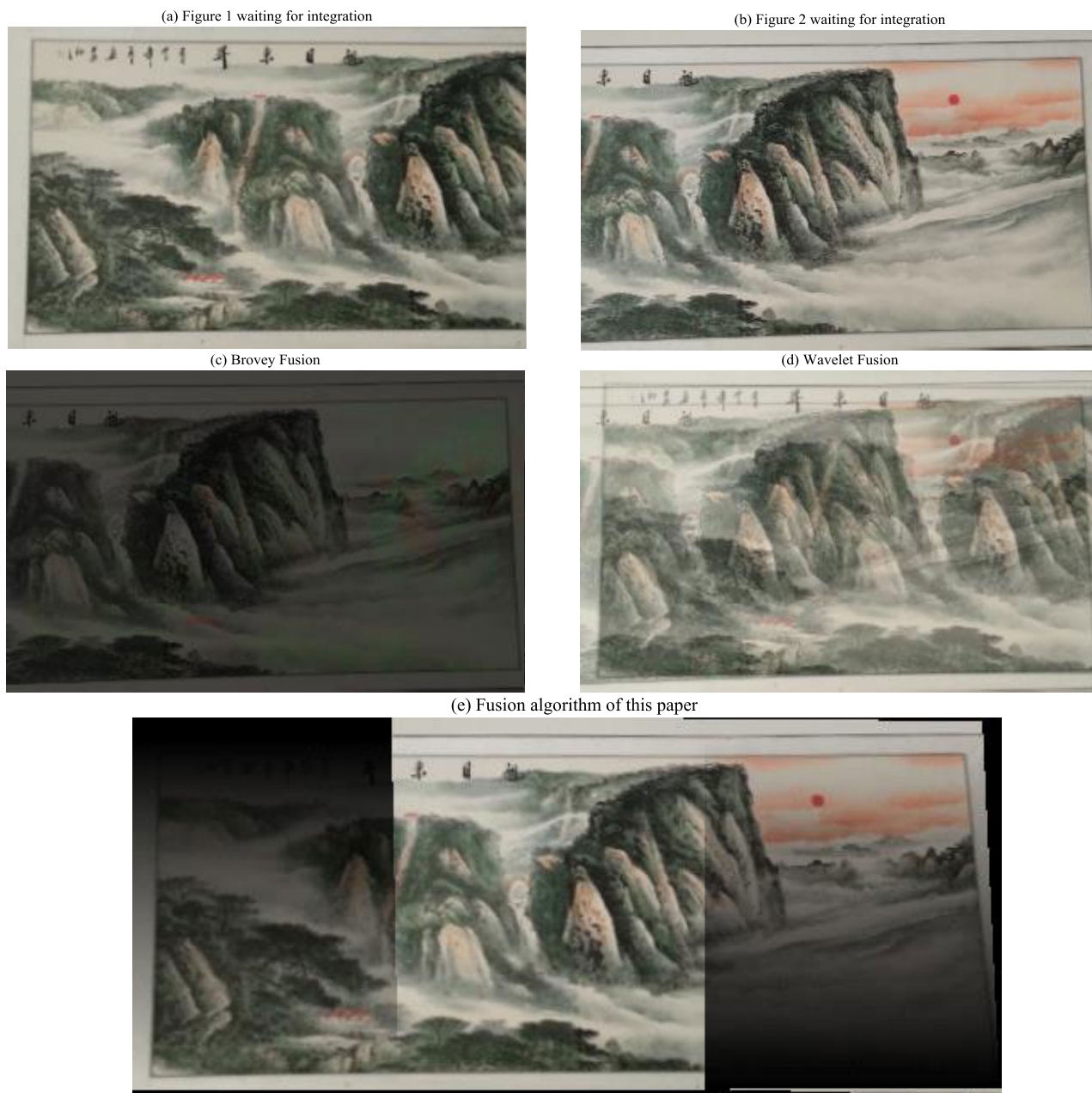
(a) Figure 1 waiting for integration

(b) Figure 2 waiting for integration

(c) Brovey Fusion

(d) Wavelet Fusion

(e) Fusion algorithm of this paper

FIGURE 15. Visualized result maps processed by multiple fusion algorithms for the sample image.

A simple visual evaluation is insufficient to prove the advantages of the method, so quantitative analysis and evaluation are still conducted. Quantitative analysis evaluates and analyzes the image color difference and gradient difference, as well as the degree of image texture information retention.

VI. CONCLUSION

This article first describes the related theoretical knowledge of image mosaicing and then describes the algorithm proposed in this article in detail. First, the SIFT algorithm is used to register an image. Second, for the disjointed case of overlapping regions, a progressive image mosaicing fusion algorithm in the form of a sine function is proposed. Finally,

segmentation technology is added to make the progressive image mosaicing fusion algorithm suitable for a variety of overlapping regions, making this algorithm a convenient and flexible image mosaicing fusion algorithm. Experimental results show that the proposed algorithm can obtain fine art fusion images superior to other fusion algorithms, which not only improves the spatial resolution of the fusion image but also maintains the consistency of the multispectral information of the image with the corresponding features so that the fusion image can better present the image details. After subjective visual comparison and objective quantitative evaluation, the fusion algorithm in this paper preserves the image color and obtains a gradient difference that is smaller than

those of other commonly used fusion algorithms. In addition, the texture difference experiment results show that the fused image obtained by the progressive fusion algorithm can well retain the texture information of the high resolution image.

REFERENCES

[1] J.-T. Zhu, C.-F. Gong, M.-X. Zhao, L. Wang, and Y. Luo, "Image mosaic algorithm based on PCA-ORB feature matching," *ISPRS Int. Arch. Photogramm., Remote Sens. Spatial Inf. Sci.*, vol. 42, pp. 83–89, Feb. 2020.

[2] C. Chang, "Fusion method of three-dimensional building construction drawing mosaic and fusion based on environmental protection engineering," *Ekoloji*, vol. 28, no. 107, pp. 3841–3852, 2019.

[3] X. Li, R. Feng, X. Guan, H. Shen, and L. Zhang, "Remote sensing image mosaicking: Achievements and challenges," *IEEE Geosci. Remote Sens. Mag.*, vol. 7, no. 4, pp. 8–22, Dec. 2019.

[4] S. Jianhui and Y. Beilei, "Research on rapid mosaic technology of UAV aerial image based on SIFT," *Comput. Appl. Softw.*, vol. 35, no. 2, pp. 230–234, 2018.

[5] Z. Yang, D. Xiang, and Y. Cheng, "VR panorama mosaic algorithm based on particle swarm optimization and mutual information," *IEEE Access*, vol. 8, pp. 134176–134184, Jul. 2020.

[6] S. Tian, "Improved electronic image stabilisation based on image mosaic and grey projection," *Rev. Comput. Eng. Stud.*, vol. 4, no. 4, pp. 108–112, Dec. 2017.

[7] L. Xin, W. Liming, W. Guitang, X. Feng, and C. Yujun, "Image mosaic method for large size component vision measurement based on homography matrix," *Comput. Meas. Control*, vol. 25, no. 11, pp. 26–29, 2017.

[8] M. Cao, Z. Deng, L. Rai, S. Teng, M. Zhao, and M. Collier, "Generating panoramic unfolded image from borehole video acquired through APBT," *Multimedia Tools Appl.*, vol. 77, no. 19, pp. 25149–25179, Oct. 2018.

[9] W. Peng, X. Hongling, L. Wenlin, and S. Wenlong, "Harris scale invariant corner detection algorithm based on the significant region," *Int. J. Signal Process., Image Process. Pattern Recognit.*, vol. 9, no. 3, pp. 413–420, Mar. 2016.

[10] Z. Wang, Y. Chen, Z. Zhu, and W. Zhao, "An automatic panoramic image mosaic method based on graph model," *Multimedia Tools Appl.*, vol. 75, no. 5, pp. 2725–2740, Mar. 2016.

[11] Y. Jia, Z. Su, W. Shen, J. Yuan, and Z. Xu, "UAV remote sensing image mosaic and its application in agriculture," *Int. J. Smart Home*, vol. 10, no. 5, pp. 159–170, May 2016.

[12] A. Pandey and U. C. Pati, "Image mosaicing: A deeper insight," *Image Vis. Comput.*, vol. 89, pp. 236–257, Sep. 2019.

[13] R.-F. Cooper, G. K. Aguirre, and J.-I.-W. Morgan, "Fully automated estimation of spacing and density for retinal mosaics," *Transl. Vis. Sci. Technol.*, vol. 8, no. 5, p. 26, Oct. 2019.

[14] Y. Tang, J. Zhang, M. Yue, X. Fang, and X. Feng, "Temperature and deformation measurement for large-scale flat specimens based on image mosaic algorithms," *Appl. Opt.*, vol. 59, no. 10, pp. 3145–3155, 2020.

[15] C. Du, J. Yuan, J. Dong, L. Li, M. Chen, and T. Li, "GPU based parallel optimization for real time panoramic video stitching," *Pattern Recognit. Lett.*, vol. 133, pp. 62–69, May 2020.

[16] Y. Huang, Y. Quan, Y. Xu, R. Xu, and H. Ji, "Removing reflection from a single image with ghosting effect," *IEEE Trans. Comput. Imag.*, vol. 6, pp. 34–45, Feb. 2020.

[17] F. Zeng, A. Jacobson, D. Smith, N. Boswell, T. Peynot, and M. Milford, "TIMTAM: Tunnel-image texturally accorded mosaic for location refinement of underground vehicles with a single camera," *IEEE Robot. Autom. Lett.*, vol. 4, no. 4, pp. 4362–4369, Oct. 2019.

[18] S. Kim and J. B. Ra, "Dynamic focal plane estimation for dental panoramic radiography," *Med. Phys.*, vol. 46, no. 11, pp. 4907–4917, Nov. 2019.

[19] H. D. Han and J. K. Han, "Modified seam finding algorithm based on saliency map to generate 360 VR image," *J. Broadcast Eng.*, vol. 24, no. 6, pp. 1096–1112, 2019.

[20] T. Liao, J. Chen, and Y. Xu, "Quality evaluation-based iterative seam estimation for image stitching," *Signal, Image Video Process.*, vol. 13, no. 6, pp. 1199–1206, Sep. 2019.

[21] J. Hamwood, D. Alonso-Caneiro, D. M. Sampson, M. J. Collins, and F. K. Chen, "Automatic detection of cone photoreceptors with fully convolutional networks," *Transl. Vis. Sci. Technol.*, vol. 8, no. 6, p. 10, Nov. 2019.

[22] W.-M. Adams, "Geographies of conservation II: Technology, surveillance and conservation by algorithm," *Prog. Hum. Geogr.*, vol. 43, no. 2, pp. 337–350, Apr. 2019.

[23] K. Sitara and B.-M. Mehtre, "Automated camera sabotage detection for enhancing video surveillance systems," *Multimedia Tools Appl.*, vol. 78, no. 5, pp. 5819–5841, Mar. 2019.

[24] H. Yong, J. Huang, W. Xiang, X. Hua, and L. Zhang, "Panoramic background image generation for PTZ cameras," *IEEE Trans. Image Process.*, vol. 28, no. 7, pp. 3162–3176, Jan. 2019.

[25] S.-S. Lin, J.-Y. Yang, H.-S. Syu, C.-H. Lin, and T.-W. Pai, "Automatic generation of puzzle tile maps for spatial-temporal data visualization," *Comput. Graph.*, vol. 82, pp. 1–12, Aug. 2019.

[26] L. Zhang, Q. Yang, Q. Sun, D. Feng, and Y. Zhao, "Research on the size of mechanical parts based on image recognition," *J. Vis. Commun. Image Represent.*, vol. 59, pp. 425–432, Feb. 2019.

[27] J. Tang, Y. Liang, F. Guo, Z. Wu, and X. Xiao, "Sequential far infrared image mosaic using coarse-to-fine scheme," *IEEE Access*, vol. 7, pp. 70185–70199, May 2019.

[28] N. Li, R. Wang, Y. Deng, T. Zhao, W. Wang, and H. Zhang, "Processing sliding mosaic mode data with modified full-aperture imaging algorithm integrating scalloping correction," *IEEE J. Sel. Topics Appl. Earth Observ. Remote Sens.*, vol. 10, no. 5, pp. 1804–1812, May 2017.

[29] M. Zheng, S. Zhou, X. Xiong, and J. Zhu, "A novel orthoimage mosaic method using the weighted A* algorithm for UAV imagery," *Comput. Geosci.*, vol. 109, pp. 238–246, Dec. 2017.

[30] L. Wei, H. Dong, J. Zhao, and G. Zhou, "Optimization model establishment and optimization software development of gas field gathering and transmission pipeline network system," *J. Intell. Fuzzy Syst.*, vol. 31, no. 4, pp. 2375–2382, Sep. 2016.

[31] P. Yugendar and K. V. R. Ravishankar, "Crowd behavioural analysis at a mass gathering event," *J. KONBiN*, vol. 46, no. 1, pp. 5–20, Jun. 2018.

[32] S. Li, X. Kang, L. Fang, J. Hu, and H. Yin, "Pixel-level image fusion: A survey of the state of the art," *Inf. Fusion*, vol. 33, pp. 100–112, Jan. 2017.

[33] X. Liu, C. Deng, J. Chanussot, D. Hong, and B. Zhao, "StfNet: A two-stream convolutional neural network for spatiotemporal image fusion," *IEEE Trans. Geosci. Remote Sens.*, vol. 57, no. 9, pp. 6552–6564, Sep. 2019.

[34] Z.-A. Yu, L.-B. Yu, S.-C. Peng, Y.-A. Han, X. Zhao, and L. Zhang, "IFCNN: A general image fusion framework based on convolutional neural network," *Inf. Fusion*, vol. 54, pp. 99–118, Feb. 2020.

[35] T. Zhang, R. Zhao, and Z. Chen, "Application of migration image registration algorithm based on improved SURF in remote sensing image mosaic," *IEEE Access*, vol. 8, pp. 163637–163645, Sep. 2020.

[36] Y. Liu, L. Wang, J. Cheng, C. Li, and X. Chen, "Multi-focus image fusion: A survey of the state of the art," *Inf. Fusion*, vol. 64, pp. 71–91, Dec. 2020.

[37] Y. Zhang and Y. Yang, "The least square optimization in image mosaic," *Proc. SPIE*, vol. 9446, Mar. 2015, Art. no. 94462Y, doi: 10.1117/12.2181212.

[38] L. Yan, J. Cao, S. Rizvi, K. Zhang, Q. Hao, and X. Cheng, "Improving the performance of image fusion based on visual saliency weight map combined with CNN," *IEEE Access*, vol. 8, pp. 59976–59986, Mar. 2020.

[39] A. M. Sharma, A. Dogra, B. Goyal, R. Vig, and S. Agrawal, "From pyramids to state-of-the-art: A study and comprehensive comparison of visible–infrared image fusion techniques," *IET Image Process.*, vol. 14, no. 9, pp. 1671–1689, Jul. 2020.

[40] H. R. Ramya and B. K. Sujatha, "Real time image fusion based technique for medical images," *J. Comput. Theor. Nanosci.*, vol. 17, no. 9, pp. 4500–4508, Jul. 2020.

BIN SONG was born in Henan, China, in 1984. She received the bachelor's and master's degrees from Jing De Zhen Ceramic University, in 2007 and 2010, respectively. She is currently pursuing the Ph.D. degree with University Putra Malaysia. She currently works with Pingdingshan University. Her research interests include ceramic design and fine arts.

● ● ●